Electronic Supplementary Material (ESI) for Sustainable Energy & Fuels.

Supplementary Information

Noncovalent Interactions Induced Self-Association in Anthraquinone-Iron Aqueous Redox Flow Batteries

Lixing Xia[1], Yujing Zhang[2], Heng Zhang[1], Shan Jiang[1], Qianglong Lv[2], Wenbo Huo[2], Fengming Chu[2], Fuzhi Wang[1], Hui Li[2,] and Zhan'ao Tan[2,*]*

[1] State Key Laboratory of Alternate Electrical Power System with Renewable Energy Sources, North China Electric Power University, Beijing 102206, China.

[2] Beijing Advanced Innovation Center for Soft Matter Science and Engineering, Beijing University of Chemical Technology, Beijing 100029, China.

Corresponding Author

* tanzhanao@mail.buct.edu.cn

* hli@mail.buct.edu.cn

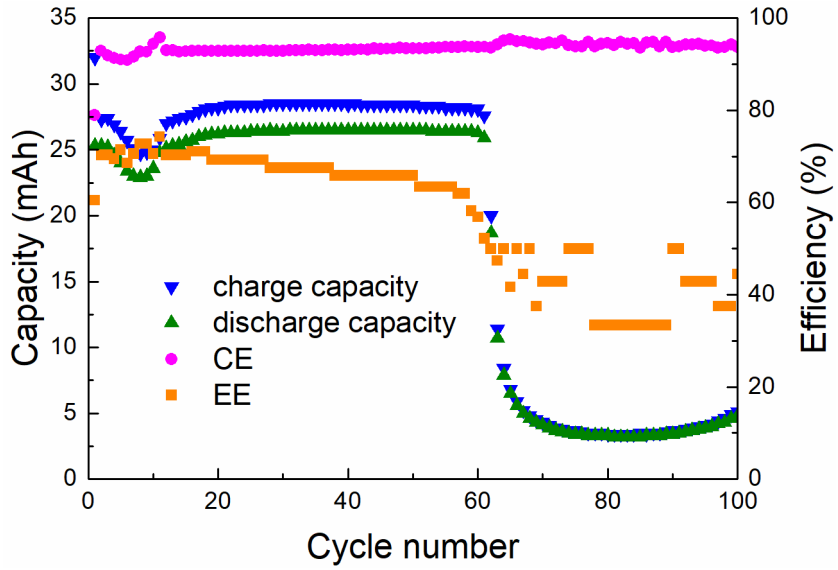

Figure S1. The anthraquinone-iron RFB was tested under 40 mA·cm^{-2} without using glycine as the acid additive.

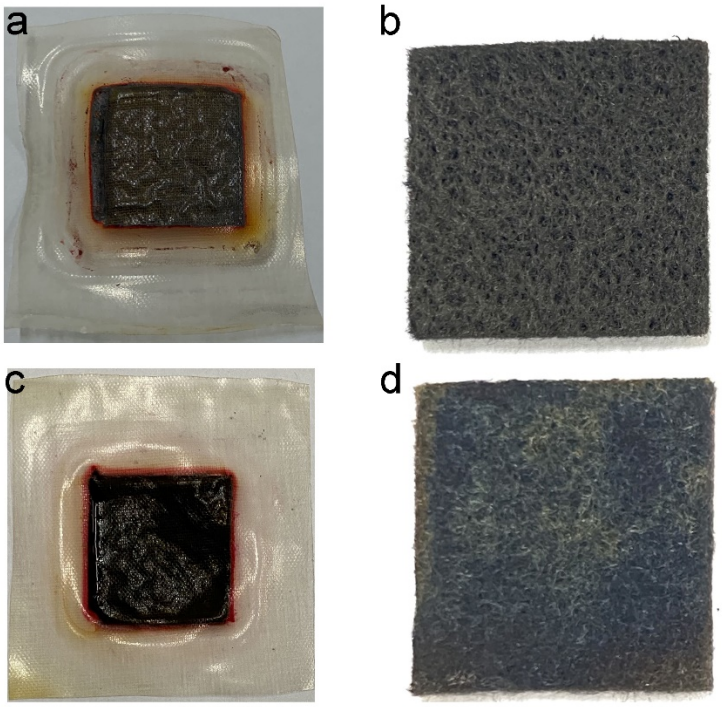

Figure S2. Images of (a) membrane and (b) carbon felt on the positive side after cycling in 0.1 M anthraquinone flow battery. Photographs of (c) membrane and (d) carbon felt on the positive side after cycling in 0.5 M anthraquinone flow battery.

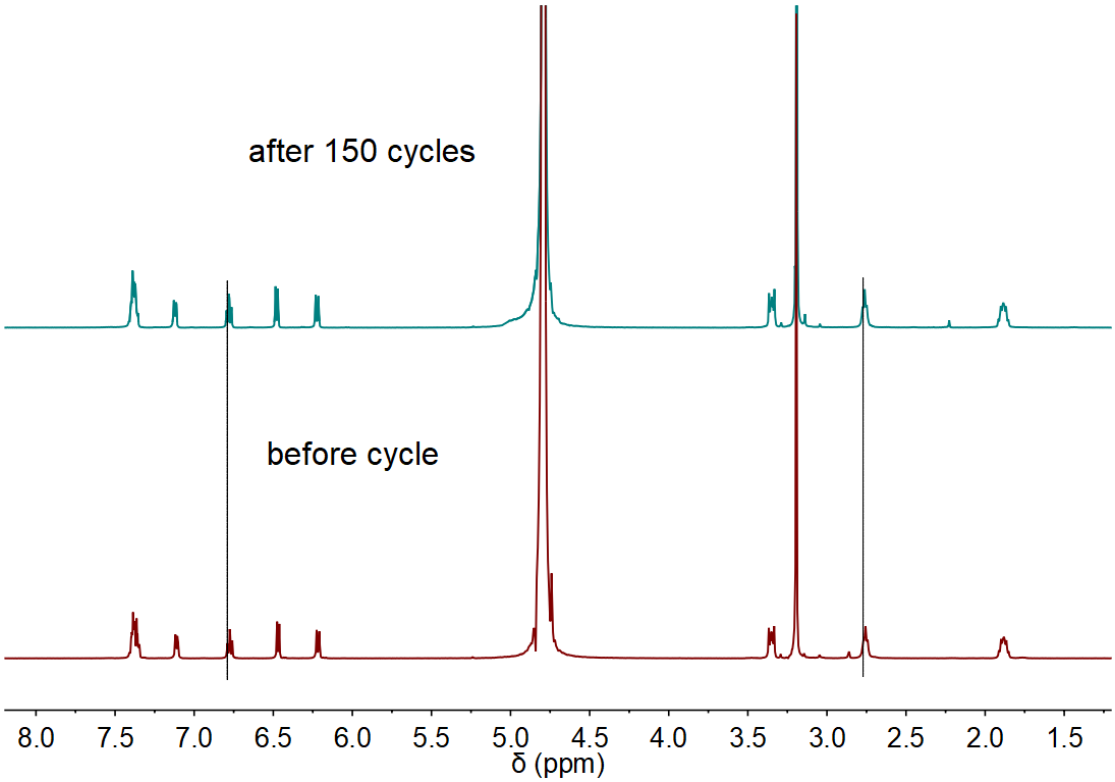

Figure S3. ^{1}H NMR spectrum (500 MHz) of 28 μL negative electrolyte in 0.55 mL D_2O before cycle (bottom) and after 150 cycles (top). The chemical shifts moved downfield slightly after 150 cycles, suggesting the concentration decreased accordingly.

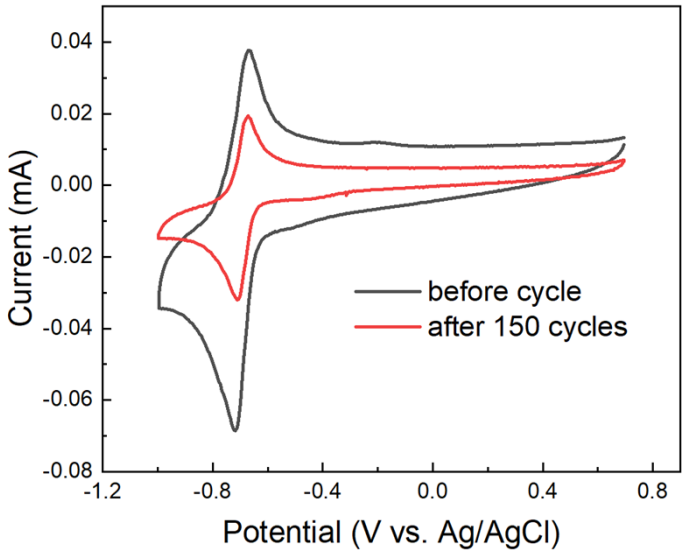

Figure S4. CV curves of 100 μL negative electrolyte dissolving in 50 mL 1 M KCl before (black line) and after 150 cycles (red line).

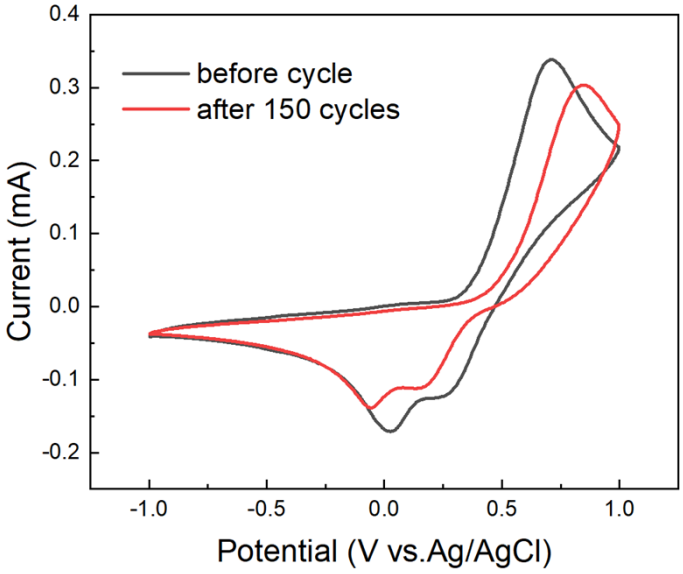

Figure S5. CV curves of 1112 µL positive electrolyte in 50 mL 1 M KCl before (black line) and after 150 cycles (red line).

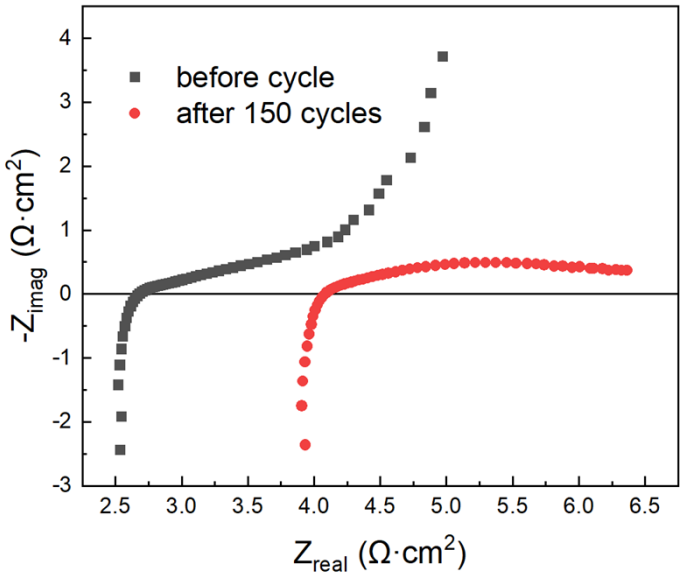

Figure S6. Nyquist plot of the 0.5 M anthraquinone-iron RFB before (black dots) and after cycling (red dots). The frequency arranges from 500 kHz to 1 Hz.

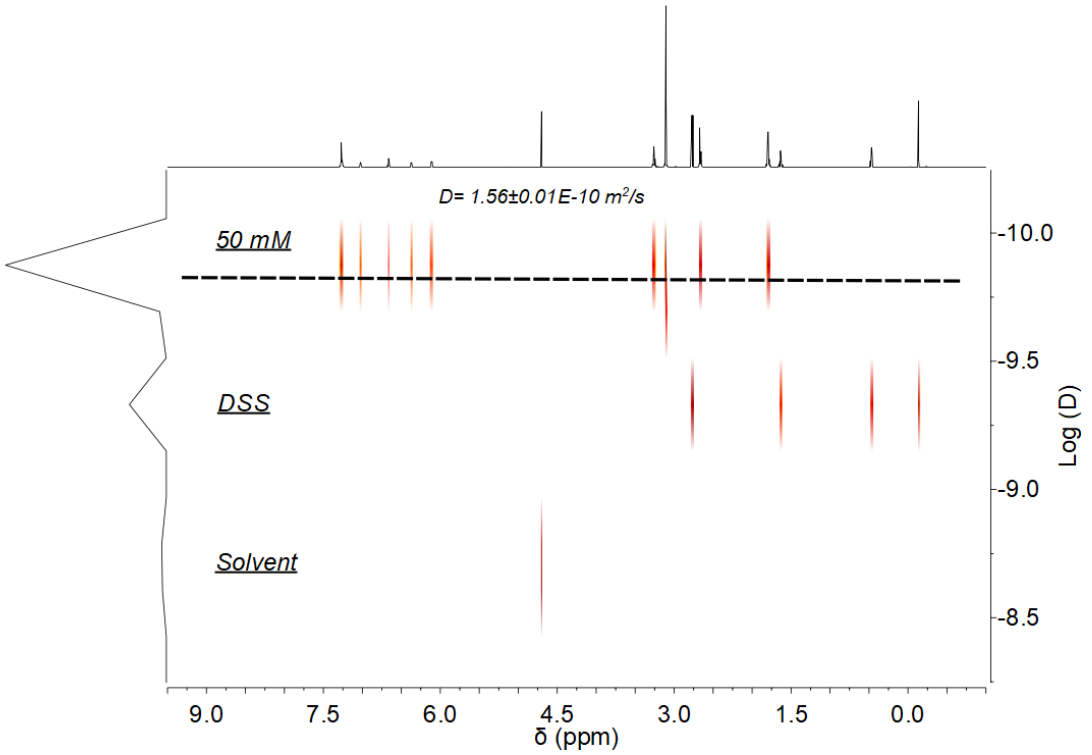

Figure S7. ^{1}H DOSY (600 MHz) spectrum of 50 mM 1-DPAQCl in D_2O at 298 K.

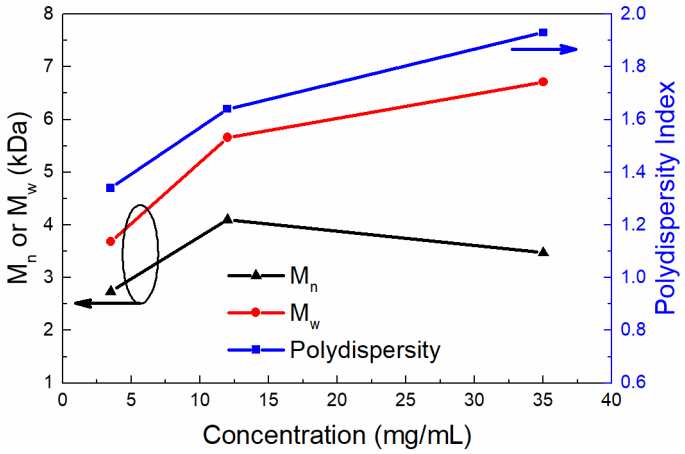

Figure S8. Number-average molecular weight (M_n), weight-average molecular weight (M_w), and polydispersity index determined by GPC versus the concentration at 3.5, 12, 35 mg·mL^{-1}.

Figure S8 displayed that M_w increased with the concentration ranging from 3.5 to 35 mg·mL^{-1}. However, M_n first increased to 4.10 kDa when the concentration was 12 mg·mL^{-1}, and then decreased to 3.47 kDa as the concentration was 35 mg·mL^{-1}. We attribute this trend to the polydispersity broadening.